Electronic Supplementary Material (ESI) for Journal of Materials Chemistry A.
This journal is © The Royal Society of Chemistry 2022

Supporting Information

Graphene Oxide Wrapped Hollow Mesoporous Carbon Spheres as A Dynamically Bipolar Composite Host for Lithium-Sulfur Batteries

Rongjie Zhe [a,1], Ting Zhu [a,b,1], Xianhe Wei [c,1], Yuanfu Ren [a], Chen Qing [a], Neng Li [c,d], Hong-En Wang [a,b,*]

[a] College of Physics and Electronics Information, Yunnan Key Laboratory of Optoelectronic Information Technology, Yunnan Normal University, 650500 Kunming, Yunnan Province, PR China. Email: hongen.wang@outlook.com

[b] Key Laboratory of Advanced Technique & Preparation for Renewable Energy Materials, Ministry of Education, Yunnan Normal University, 650500 Kunming, Yunnan Province, PR China. Email: hongen.wang@ynnu.edu.cn

[c] State Key Laboratory of Silicate Materials for Architectures, Wuhan University of Technology, 430070 Wuhan, Hubei Province, PR China.

[d] International Cooperation on Designer Low-Carbon & Environmental Materials (CDLCEM), School of Materials Science and Engineering, Zhengzhou University, 450001 Zhengzhou, Henan, China.

[1] These authors contributed equally to this work.

Experimental

Materials Synthesis.

Synthesis of precursor. 3.5 mL of tetrapropoxysilane (TPOS) was added into a mixture of 140 mL absolute ethanol (C_2H_6O), 20 mL deionized water and 6 mL ammonia solution (25 wt.%) along with stirring. Then, 0.4 g resorcinol and 0.56 mL formaldehyde solution (37wt.%) was added into the above solution along with stirring for another 20 h. During this period, the reaction system gradually changed from colorless transparent solution to brownish yellow suspension. After reaction, the as-obtained product was centrifuged and washed with water and ethanol three times, respectively, followed by drying in an oven at 60 ℃ for 12 h.

Carbonization of the precursor. The precursor was carbonized at 800 ºC for 5 h in a tube furnace purged in Ar with a heating rate of 2 ℃ min^{-1}. Then, the resultant product consisting of carbon spheres@SiO_2 was naturally cooled to room temperature.

Fabrication of hollow carbon spheres with mesoporous shells (HMCS). The carbon@SiO_2 composite was dispersed in a 4 M NaOH solution under sonication, then soaked for 12 h, followed by rinsing thoroughly with deionized water and filtering, and finally drying it in an oven at 60 ℃ for 12 h.

Synthesis of HMCS/S Composites. 150 mg sulfur powders were dissolved into 5 mL CS_2 by stirring, followed by addition of 50 mg HMCS material. The resultant mixture was sonicated for 30 min to get a good dispersion of each species, followed by

drying 60 ℃ for 12 h in an oven to allow the full volatilization of CS_2 solvent to obtain a composite sample containing HMCS and S. Next, the sample was transferred in a sealed stainless-steel autoclave with a PTFE liner place and and maintained at 155 ºC for 12 h to obtain the final HMCS/S composite.

Synthesis of HMCS/@GO composite. 100 mg HMCS/S sample was dispersed into 100 mL deionized water containing 2 mL Triton-X-100 as dispersant by sonication for 1 h. 25 mg commercial graphene oxide (GO) flakes were dispersed into 30 mL deionized water by sonication for 2 h. Then, the as-obtained GO solution was poured into the mixture of HMCS/S, deionized and Triton-X-100 along with stirring for 1 h, followed by filtering, washing, and freeze-drying for 20 h to obtain the HMCS/S@GO composite sample.

Materials Characterization.

The surface morphologies of the samples were observed by a scanning electron microscope (SEM, Hitachi S-4800). Transmission electron microscopy images were acquired on a JEM-2100F transmission electron microscope operated at an acceleration voltage of 200 kV. Powder X-ray diffraction patterns (XRD) of the samples were recorded on a Bruker X-ray diffractometer with Cu Kα irradiation at 40 kV and 40 mA. The elemental composition and electronic states of corresponding elements on the samples' surface were analyzed using an X-ray photoelectron spectroscope (XPS, ThermoFisher Scientific, alpha) employing a monochromatic Al Kα radiation source at 15 kV. The positions of XPS peaks were calibrated with C 1s peak of an adventitious

carbon tape at 284.8 eV as reference. Raman spectra of the samples were recorded on an INVIA (RENISHAW corp.) laser Raman spectroscope with an excitation wavelength of 633 nm. Fourier transform infrared (FTIR) spectra were collected on a spectrometer (Nexus, Thermo Nicolet corp.) using KBr pellets within a wavenumber range of 400~4000 cm^{-1}. The specific surface area and pore diameter distribution data were determined by Brunner-Emmett-Teller (BET) and Barrett-Joyner-Halenda (BJH) methods, respectively using N_2 adsorption/desorption isotherms acquired at 77 K on a Tri Star II 3020 surface area and porosity analyzer. Before adsorption experiments, the samples were outgassed at 100 ºC for 24 h under a vacuum line. Thermogravimetric (TG) analyses were performed on a Pyris 1 thermogravimetric analyzer with a heating rate of 5 ºC min^{-1} in N_2 atmosphere to determine the sulfur content.

Electrode fabrication and electrochemical cell assembly.

The active materials (HMCS/S@GO or HMCS/S), conductive carbon additive (super P), and polyvinylidene fluoride (PVDF) binder with a weight ratio of 8:1:1 were blended and ground in N-methylpyrrolidone (NMP) solvent to get a homogeneous slurry. The slurry was spread onto an Al foil by a doctor-blading method, followed by drying at 55 ºC for 12 h in vacuum and then cutting into circular disks with a dimeter of 12 mm for further use. The sulfur loading in the cathode is *ca.* 1 mg/cm^2.

The lithium-sulfur batteries were assembled with the HMCS/S@GO (or HMCS/S) coated Al disks as a cathode, a lithium foil as anode, Celgard-2400 as a separator, and bis(trifluoromethane) sulfonimide lithium salt (LiTFSI) dissolved in ethylene glycol

dimethyl ether (DME) and 1,3-dioxyclopentane (DOL) with a volume ratio of 1:1 as the working electrolyte. 0.1 M $LiNO_3$ was added into the electrolyte as an additive. The cell assembling was carried out in an Ar-purged glovebox with water and O_2 contents below 0.1 ppm.

Electrochemical measurements.

Cyclic voltammetry (CV) sweeps were recorded on a CHI660D (Chenhua, Shanghai) electrochemical working station within a potential range of 1.4~2.8 V vs. Li^+/Li. Galvanostatic charge/discharge (GCD) profiles were obtained on a LAND CT2001A multichannel battery testing system within a potential window of 1.4~2.8 V vs Li^+/Li at different current densities (1 C = 1675 mA g^{-1}). Electrochemical impedance spectra (EIS) were collected on an Autolab PGSTAT 302N electrochemical working station at open-circuit potential within a frequency range from 100 kHz to 0.1 Hz. All the electrochemical tests were performed at room temperature.

Molecular dynamics (MD) simulations.

Classical MD simulations were performed using the Forcite module implemented in Materials Studio. The force field parameters were obtained from the COMPASS force fields. NVT ensemble at 300 K with COMPASS force field. The size of the graphene sheet is ~6.2 × 6.9 nm^2 comprised of 1734 C atoms and surface passivated by 116 H atoms. An amorphous carbon sphere with a radius of ~1.6 nm containing 2431 C atoms was cut from an amorphous carbon supercell and used to model the dynamic properties of carbon spheres. Geometry optimizations were first performed to get the most stable

structures for the graphene sheet and amorphous carbon sphere. Then, the carbon sphere was put above the graphene sheet with a vertical distance of 6.2 Å as an initial configuration for MD simulation. Both the electrostatic and Van der Waals interactions were considered on an atom-based summation method with a cutoff length of 12.5 Å. A NVT ensemble was adopted with Nose thermostat. The integration time step was 1 fs. The system was maintained at 300 K over a total period of 30 ps with a random initial speed for all the atoms. The system can gradually reach equilibrium within the first 15 ps.

First-principles density functional theory (DFT) calculations.

The electronic structures and energetics of the molecules and surfaces were simulated using the Dmol3 program in Materials Studio with density functional theory (DFT) framework.[1] DFT-D with the Grimme dispersion correction method was adopted to correct the van der Waals forces in all calculations.[2] Perdew, Burke and Enzerhof (PBE) with generalized gradient corrected (GGA) functional were used to account for the exchange and correlation interactions.[3] Double numerical plus polarization (DNP) basis set with a fine quality was employed with hexadecapole for multipolar expansion. Numerical basis set and exact DFT spherical atomic orbitals can minimize the basis set superposition (BSSP) effects and obtain a good description even for weak bonds. [4] The fine settings and thermal smearing of 0.01 Hartree were used to acquire accurate quantitative results and speed up convergence. The adsorption energies (E_{ads}) were determined by the following formula:

$$E_{ads} = E_{mol/sub} - E_{sub} - E_{mol}$$

Where $E_{mol/sub}$, E_{sub} and E_{mol} represent the total ground state electronic energies of the substrate with adsorbed molecules, the pure substrate and the pure molecules in vacuum, respectively. Energetically, a negative E_{ads} value is desirable for a surface adsorption process.

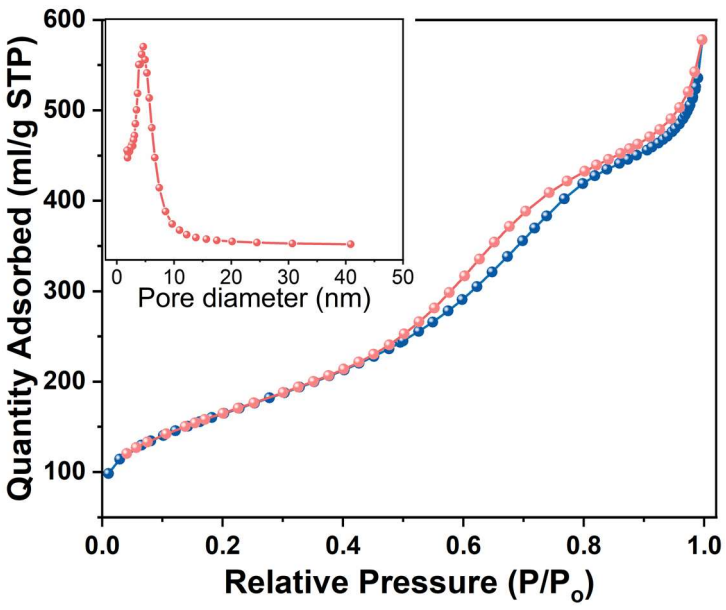

Figure S1. N_2 adsorption/desorption isotherms and pore size distribution curves of the HMCS sample.

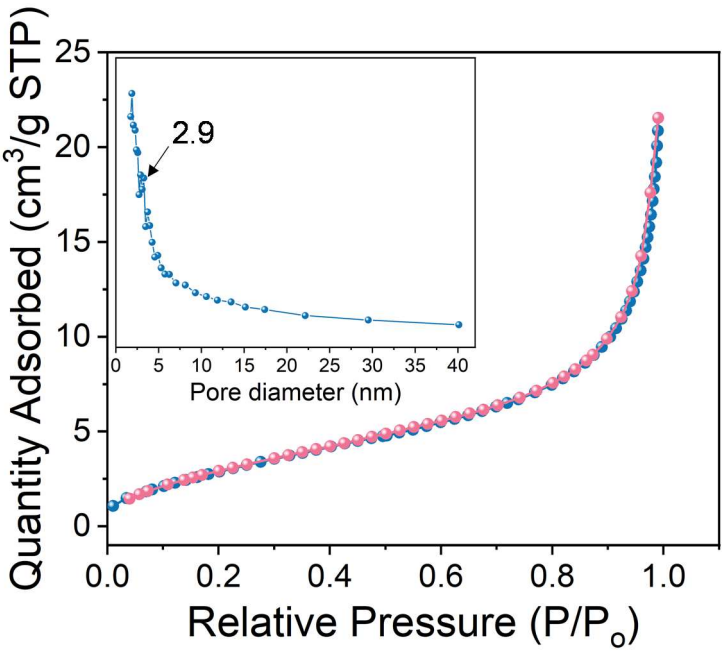

Figure S2. N_2 adsorption/desorption isotherms and pore size distribution of the HMCS/S product.

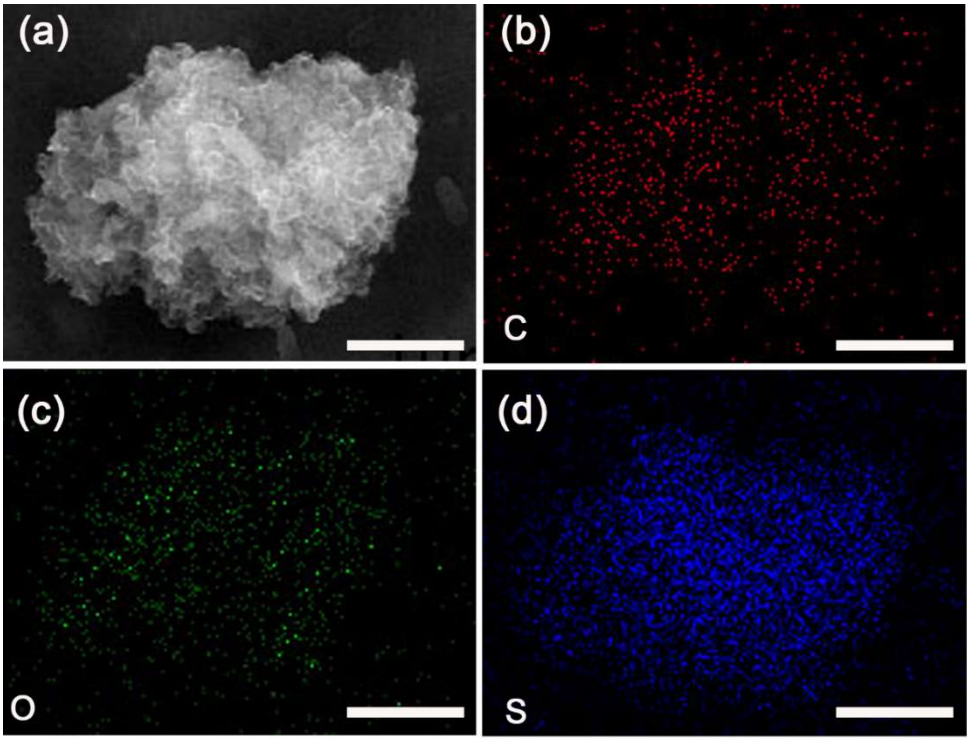

Figure S3. (a) SEM image of HMCS/S and corresponding energy-dispersive X-ray (EDX) mapping images of (b) C, (c) S and (d) O elements, respectively, demonstrating the homogeneous distribution of the three elements. Scale bar: 1 μm.

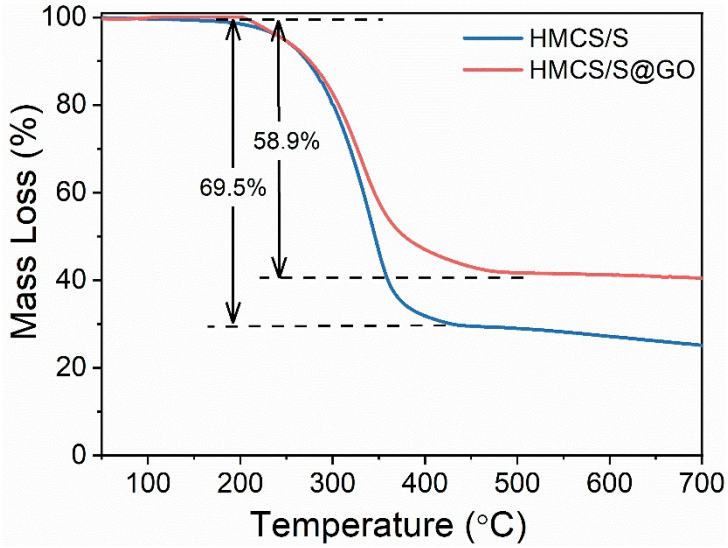

Figure S4. Thermogravimetric analysis curves of HMCS@GO and HMCS/S, respectively.

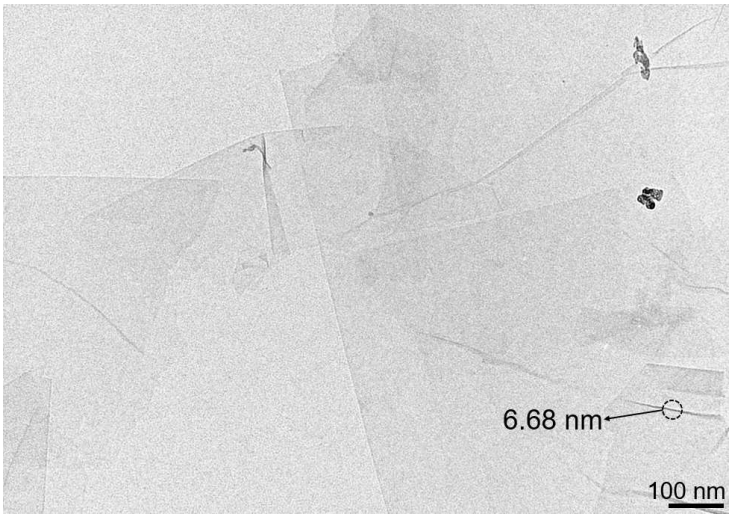

Figure S5. TEM micrograph of graphene oxide sheets dispersed in ethanol by sonication.

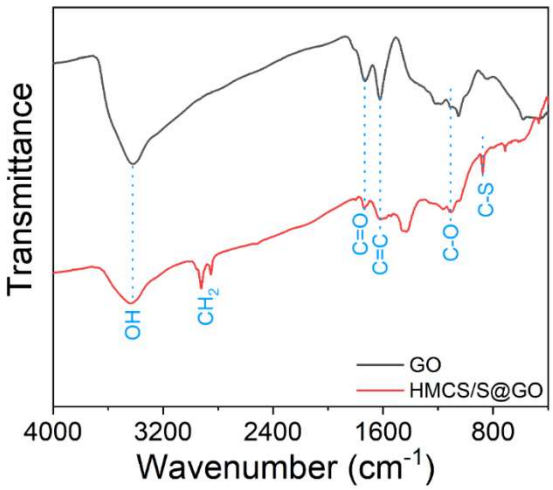

Figure S6. FTIR spectra of pure GO (black) and HMCS/S@GO sample (red), respectively.

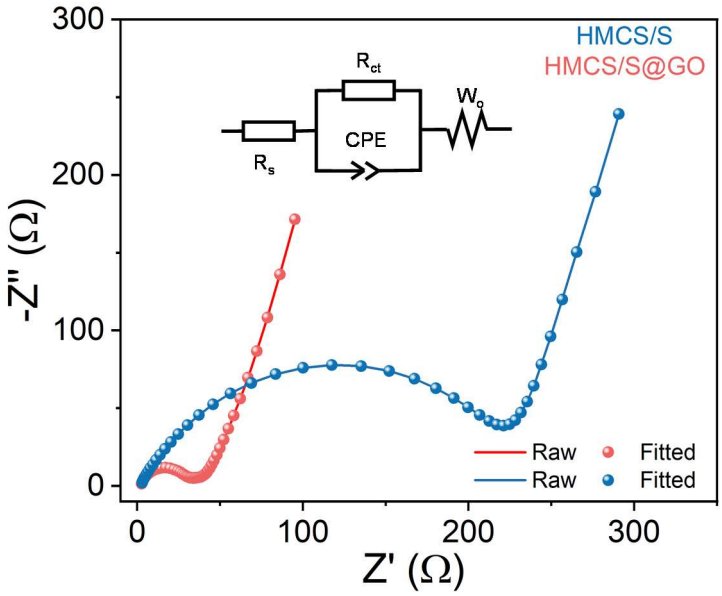

Figure S7. EIS spectra of the HMCS@GO (a) and HMCS/S (b) electrodes, respectively.

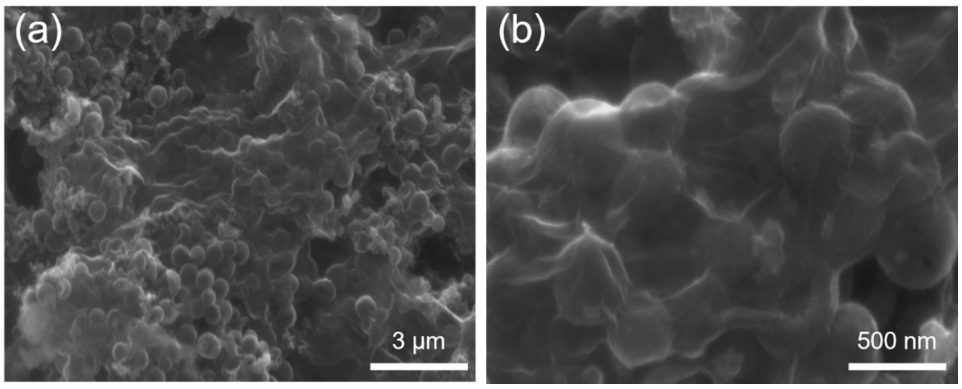

Figure S8. SEM images of the HMCS/S@GO electrode after 100 cycles at 1 C.

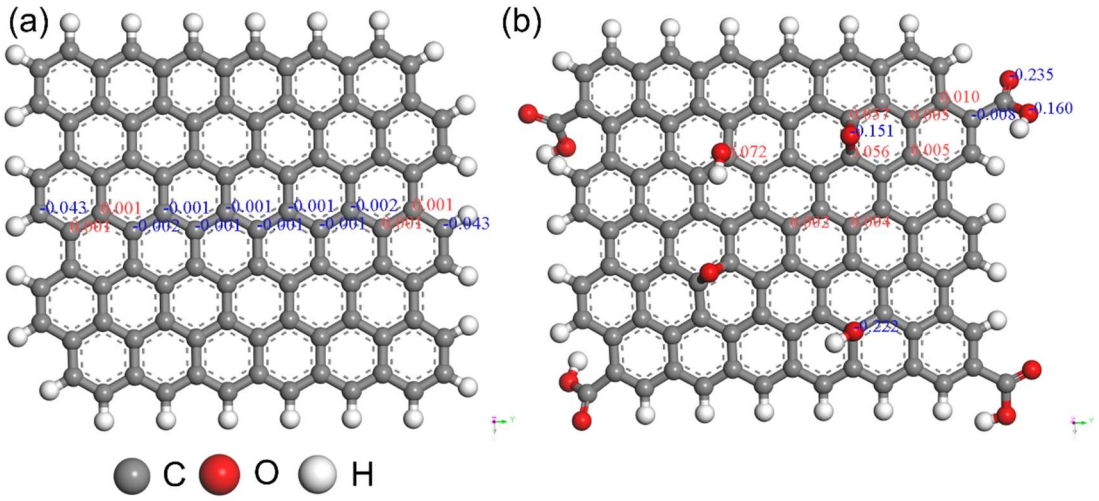

Figure S9. Optimized geometry configurations of (a) a graphene sheet and (b) a graphene oxide sheet with Hirshfeld charge distribution labelled on several selected atoms.

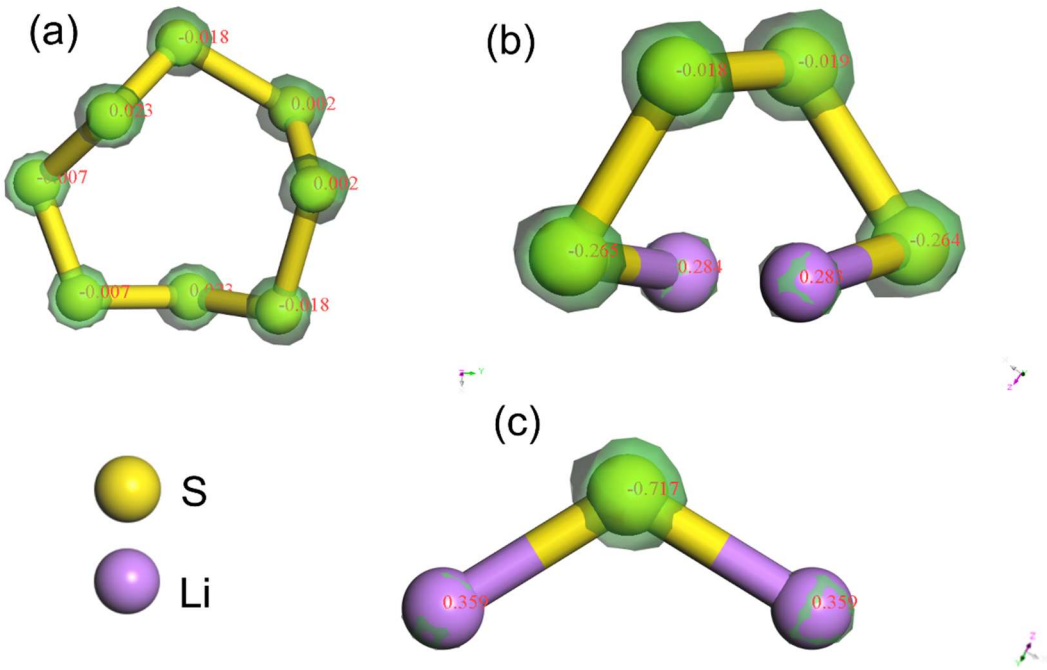

Figure S10. Optimized geometry structures of a S_8 molecule (a), Li_2S_4 molecule (b), and Li_2S molecule (c) with charge density distribution contours (in green) and Hirshfeld charge distribution.

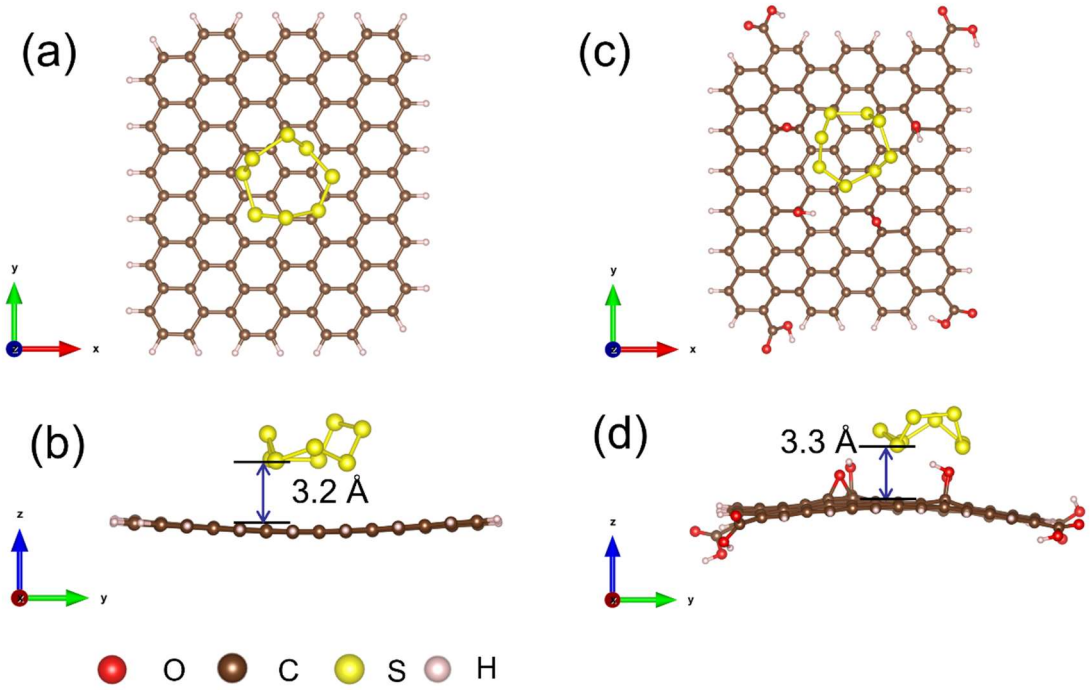

Figure S11. Optimized geometry configurations of a S_8 molecule adsorbed on (a, b) pristine graphene and (c, d) graphene oxide sheets, respectively, yielding an adsorption energy (E_{ads}) of -2.19 and -2.55 eV, respectively.

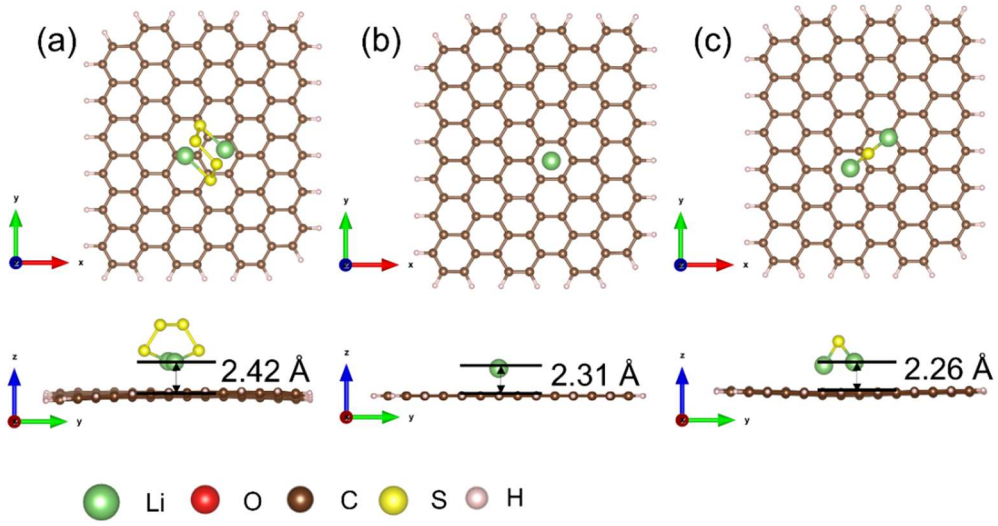

Figure S12. Optimized geometry structures of a Li_2S_4 molecule, Li^+ and Li_2S molecule adsorbed on a graphene sheet, yielding an E_{ads} of -1.39, -3.23 and -2.21 eV, respectively.

Table S1. Brief comparison of electrochemical performance of current work with recently relevant literature.

Cathode Host	Capacity (mAh/g, 0.2 C)	Capacity (mAh/g, 0.5 C)	Capacity (mAh/g, 1 C)	Capacity (mAh/g, 2 C)	**Ref.**
HMCS/S@GO	**976**	**842**	**739**	**626**	**This work**
sepiolite	884	627	381	NA	[5]
Ti_4O_7 microspheres	NA	780	630	510	[6]
$Bi_2S_3/Bi_2O_{2.33}$@C	NA	817	697	547	[7]
TiO_2@PP_y	749.9	637.5	585.5	402.0	[8]
Cationic COFs	905	828	771	696	[9]
C/TiS_x	893	685	521	424	[10]
chitosan@rGO	912	655	487	341	[11]
micro/mesoporous C	795	717	596	427	[12]
hollow C/PEDOT:PSS	1001	789	703	620	[13]
CMK3	888	798	660	550	[14]
C/Co_3S_4 polyhedron	1057.6	788.9	592.1	NA	[15]
MnO_2@C@$Ti_3C_2T_x$	895	789	740	688	[16]

NA: not available

References

1. B. Delley, *Theoret. Computation. Chem.*, 1995, **2**, 221-254.
2. S. Grimme, *J. Comput. Chem.*, 2006, **27**, 1787-1799.
3. J. P. Perdew, K. Burke and M. Ernzerhof, *Phys. Rev. Lett.*, 1997, **78**, 1396-1396.
4. B. Delley, *J. Chem. Phys.*, 1990, **92**, 508-517.
5. C. Kalaiselvi, K. Krishnaveni, V. Priyanka, P. Rajkumar, R. Subadevi and M. Sivakumar, *Ceram. Int.*, 2021, **47**, 692-699.
6. M. Liu, S. Jhulki, Z. Sun, A. Magasinski, C. Hendrix and G. Yushin, *Nano Energy*, 2021, **79**.
7. L. Jia, J. Wang, S. Ren, G. Ren, X. Jin, L. Kao, X. Feng, F. Yang, Q. Wang, L. Pan, Q. Li, Y. s. Liu, Y. Wu, G. Liu, J. Feng, S. Fan, Y. Ye, J. Guo and Y. Zhang, *Energy Environ. Mater.*, 2020, **4**, 222-228.
8. H. Song, H. Yuan, H. Chen, A. Tang, G. Xu, L. Liu, Z. Zhang and Q. Kuang, *J. Solid State Electrochem.*, 2020, **24**, 997-1006.
9. S. Wang, Y. Liang, T. Dai, Y. Liu, Z. Sui, X. Tian and Q. Chen, *J. Colloid Interf. Sci.*, 2021, **591**, 264-272.
10. Y. Yao, Y. Wu, N. Wang, M. Li and T. Hang, *Mater. Chem. Phys.*, 2021, **258**.
11. Z. Jiang, L. Chen, W. Zhang, S. Chen, X. Jian, X. Liu, H. Chen, C. Guo and W. Li, *Energy*, 2021, **220**.
12. H. Liu, M. Chen, P. Zeng, X. Li, J. Luo, Y. Li, T. Xing, B. Chang, X. Wang and Z. Luo, *ACS Sustain. Chem. Eng.*, 2019, **8**, 351-361.
13. Y. Ren, J. Hu, H. Zhong and L. Zhang, *J. Alloy. Compd.*, 2020, **837**.
14. H. Liu, P. Zeng, Y. Li, H. Yu, M. Chen, Z. Luo, C. Miao, G. Chen and X. Wang, *J. Alloy. Compd.*, 2020, **835**.
15. J. Wei, C. Jiang, B. Chen and H. Zhang, *Fullerenes, Nanotubes and Carbon Nanostructures*, 2021, **30**, 392-403.
16. H. Zhang, P. Zhang, L. Pan, W. He, Q. Qi, Z. Bao, L. Yang, W. Zhang, M. W. Barsoum and Z. Sun, *Nanoscale*, 2020, **12**, 24196-24205.